

# SAMPLING AND RECONSTRUCTING SPATIAL FIELDS USING MOBILE SENSORS

Jayakrishnan Unnikrishnan and Martin Vetterli

School of Computer and Communication Sciences  
Ecole Polytechnique Fédérale de Lausanne (EPFL), CH-1015 Lausanne, Switzerland  
Email: {jay.unnikrishnan, martin.vetterli}@epfl.ch

## ABSTRACT

The classical approach to sampling time-invariant spatial fields uses static sensors distributed over space. We study a new approach involving mobile sensors that move through space measuring the field values along their paths. A single moving sensor can take measurements over a wide spatial area thus acting as a substitute for a potentially large number of static sensors. A moving sensor encounters the spatial field in its path in the form of a time-domain signal. Hence a time-domain anti-aliasing filter can be employed at the mobile sensor to limit the amount of out-of-band noise prior to sampling. We analytically quantify the advantage of mobile sensing over static sensing in rejecting out-of-band noise. We also demonstrate via simulations the improvement in reconstruction accuracy that can be obtained using mobile sensors and filtering in a temperature measurement problem.

**Index Terms**— Spatial sampling, mobile sensing, anti-aliasing filtering, spatial smoothing.

## 1. INTRODUCTION

Consider the problem of sampling and reconstructing a time-invariant spatial field  $\tilde{f}(r)$  where  $r \in \mathbb{R}^2$ . For example  $\tilde{f}(\cdot)$  could represent the temperature distribution in a room or the concentration level of some air-pollutant in a city. Suppose  $\tilde{f}$  can be expressed as

$$\tilde{f}(r) = f(r) + w(r), r \in \mathbb{R}^2 \quad (1)$$

where  $f \in L^2(\mathbb{R}^2)$  denotes the field of interest and  $w$  denotes non-bandlimited spatial noise. Suppose that  $f$  is spatially bandlimited. If the noise  $w$  is absent, then the field  $\tilde{f} = f$  is bandlimited, and we know from classical sampling theory [1] that we can recover it exactly from samples of the field measured by a network of uniformly spaced static sensors. In particular, the mapping  $f : \mathbb{R}^2 \mapsto \mathbb{R}$  can be reconstructed exactly from measurements of the form  $\{f(m\Delta_x, n\Delta_y) : m, n \in \mathbb{Z}\}$  taken by static sensors located on a rectangular lattice of

points, provided that the Fourier transform  $F(\cdot)$  of the field  $f$  is supported on a set  $\Omega \subset [-\frac{\pi}{\Delta_x}, \frac{\pi}{\Delta_x}] \times [-\frac{\pi}{\Delta_y}, \frac{\pi}{\Delta_y}]$ . However, if  $w \neq 0$  then the observed field  $\tilde{f}$  is not bandlimited and we expect to see some effects of spatial aliasing while sampling the field using static sensors. There is no way to implement a spatial anti-aliasing filter in a static sensing setup [2]. Although it is possible to approximate a filter by averaging across readings from neighboring sensors, such a scheme is quite expensive to implement since it requires a high spatial density of sensors. However, as we illustrate in this paper, in a mobile sensing setup it is possible to filter the observed field in time prior to sampling which induces filtering over space in the direction of motion of the sensor. This leads to a significant improvement in the effective SNR in the reconstructed field. Moreover, in some applications like pollution monitoring in a city, mobile sensing is more cost-effective than static sensing since a single mobile sensor can take field measurements over a large area, and sometimes it is the only feasible solution when static deployments are impractical.

Most works in the literature on sampling and reconstruction schemes for spatial fields have focused on static sensing (see, e.g., [1], [3]). The advantages of mobile sensing over static sensing have been noted in room impulse response measurement for communication systems [4] and in suppressing spatial aliasing in audio source localization [5]. In a different context, moving antennae have been shown to provide advantages over static antennae in synthetic aperture radar [6]. Some works on mobile sensing focus on algorithms for adaptive path-planning [7], [8]. However, the problem of sampling and reconstructing bandlimited fields using samples taken by mobile sensors has not been studied from a signal processing perspective. In a related work [9] we studied the problem of designing sampling trajectories for mobile sensing, while in this paper we illustrate some of the advantages of mobile sampling over static sampling, in particular in the presence of noise.

The paper is organized as follows. We introduce the sampling setup in Section 2 and provide a detailed comparison of the mobile and static sampling methods in Section 3. In Section 4 we present simulation results demonstrating the performance improvement with mobile sensing. In Section 5 we

---

This research was supported by ERC Advanced Investigators Grant: Sparse Sampling: Theory, Algorithms and Applications SPARSAM no 247006.

summarize our results and present avenues for future work.

## 2. MOBILE SAMPLING SETUP

### 2.1. Spatial smoothing via time-domain filtering

Let  $f \in L^2(\mathbb{R}^2)$  denote a bandlimited spatial field with Fourier transform  $F$  defined by

$$F(\omega) = \int f(r) \exp(-j\langle \omega, r \rangle), \omega \in \mathbb{R}^2$$

supported on a compact convex set  $\Omega \subset \mathbb{R}^2$ . A sensor moving through this field receives as input a time-domain signal  $s(t)$  representing the field  $f$  along the path of the sensor,

$$s(t) = \tilde{f}(r(t)) = f(r(t)) + w(r(t)) \quad (2)$$

where  $r(t) \in \mathbb{R}^2$  denotes the position of the sensor as a function of time  $t$ . It is known that if the sensor is moving at constant velocity then  $r(t)$  is an affine function of  $t$  of the form  $r(t) = r_0 + vt$ , and  $f(r(t))$  is bandlimited [9] in the sense that its Fourier transform is supported on the set  $\Omega_s := \{\langle v, \omega \rangle : \omega \in \Omega\} \subset \mathbb{R}$ . Hence, prior to sampling at the moving sensor we can pass  $s(t)$  through an anti-aliasing filter whose passband is aligned with  $\Omega_s$ . This enables us to discard the component of the out-of-band noise in the direction of motion of the sensor thus inducing *spatial smoothing*. However, a caveat to note is the peculiar fact that for 2-dimensional spatial fields such filtering allows us to perform spatial smoothing only in the direction of motion of the sensor. In other words, the anti-aliasing filters are *thin*, i.e., the effective spatial impulse response of the filter is supported on a 1-dimensional set.

### 2.2. Sampling trajectories and reconstruction

Although there are several possible choices of sensor trajectories [9] for sampling a bandlimited field, we restrict ourselves to equispaced straight lines parallel to the  $x$ -axis. Thus for each  $i \in \mathbb{Z}$  there is a sensor moving along the line  $\{(x, i\Delta_y) : x \in \mathbb{R}\}$  taking measurements along its path. Here  $\Delta_y$  represents the spatial separation between adjacent parallel trajectories. Assuming further that each mobile sensor takes filtered samples at intervals of  $\Delta_x$  spatial units we obtain samples at points of the form  $\{\Lambda n : n \in \mathbb{Z}^2\}$  where  $\Lambda = \begin{pmatrix} \Delta_x & 0 \\ 0 & \Delta_y \end{pmatrix}$ . The samples are given by the two-dimensional convolution  $\mu[n] = (\nu \star h_s)(\Lambda n), n \in \mathbb{Z}^2$ , where  $h_s$  represents the effective two-dimensional sampling kernel induced by the sampling trajectories and the filtering operation, and  $\nu$  represents the field  $\tilde{f}$ . Figure 1 shows the system of sampling and reconstruction. Here  $h_r(\cdot)$  represents the two-dimensional waveform used for reconstruction. In the sequel we assume that the field  $f$  is bandlimited to  $\Omega = [-\rho, \rho] \times [-\rho, \rho]$ . Hence we use an ideal sinc-reconstruction

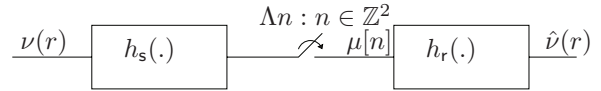


Fig. 1. Sampling and reconstruction setup.

kernel given by  $h_r(x, y) = \frac{\Delta_x \Delta_y \rho^2}{\pi^2} \text{sinc}\left(\frac{\rho x}{\pi}\right) \text{sinc}\left(\frac{\rho y}{\pi}\right)$  where  $\text{sinc}(x) := \frac{\sin(\pi x)}{\pi x}$ . The kernel has the following representation in the Fourier domain

$$H_r(\omega) = \begin{cases} \Delta_x \Delta_y & \text{for } 0 \leq |\omega_x|, |\omega_y| \leq \rho \\ 0 & \text{else} \end{cases} \quad (3)$$

where  $\omega = (\omega_x, \omega_y)^T$ . The reconstructed field is given by  $\hat{\nu}(r) = \sum_{n \in \mathbb{Z}^2} \mu[n] h_r(r - \Lambda n), r \in \mathbb{R}^2$ .

## 3. COMPARISON WITH STATIC SENSING

As we mentioned earlier, it is not possible to implement a spatial anti-aliasing filter in a static sensing setup. We now study the reduction of out-of-band noise that can be obtained by using an anti-aliasing filter in a mobile sensing scheme for sampling a bandlimited field in noise. Suppose the field of interest  $f$  is bandlimited to  $\Omega = [-\rho, \rho] \times [-\rho, \rho]$  as in Section 2.2. We represent both the static and mobile sampling schemes as shown in Figure 1 for specific choices of the parameters  $h_s$  and  $\Lambda$ . We consider a static sampling scheme that uses a rectangular sampling grid at the Nyquist sampling rate i.e.,  $\Delta_x = \Delta_y = \frac{\pi}{\rho}$ , and we consider a mobile sampling scheme as in Section 2.2 with the spacing  $\Delta_y$  between the sensor trajectories equal to the Nyquist interval  $\frac{\pi}{\rho}$ . We consider two extreme choices for the low-pass filter employed prior to sampling in the mobile sensing scheme - the ideal low-pass filter (LPF) with a sinc response, and a more practically feasible filter, the box-filter whose impulse response is a rectangular pulse.

We now study the response of the sampling schemes to noise. Suppose the input  $\nu$  in Figure 1 represents weak-sense stationary noise with spectral density  $S_\nu(\omega), \omega \in \mathbb{R}^2$ . Then the power spectral density of  $\mu$  is given by,

$$S_\mu(e^{j\omega}) = \sum_{n \in \mathbb{Z}^2} \frac{S_\nu(\Lambda^{-1}(\omega - 2\pi n)) |H_s(\Lambda^{-1}(\omega - 2\pi n))|^2}{\Delta_x \Delta_y}$$

The output signal is cyclostationary with an effective p.s.d. of

$$S_{\hat{\nu}}(\omega) = \frac{1}{\Delta_x \Delta_y} |H_r(\omega)|^2 S_\mu(e^{j\Lambda \omega}). \quad (4)$$

### 3.1. Static sampling

In the case of static sensing we do not have any spatial filtering and hence the sampling kernel is an impulse function  $h_s(x, y) = \delta(x)\delta(y)$  and is equivalently given in the Fourier domain by,

$$H_s(\omega) = 1 \text{ for all } \omega \in \mathbb{R}^2. \quad (5)$$

Since we assume Nyquist rate sampling we also have  $\Delta_x = \Delta_y = \frac{\pi}{\rho}$ . Substituting (5) in (4) and integrating we obtain the following expression for the noise variance  $\sigma_{stat}^2$ :

$$\sigma_{stat}^2 = \frac{1}{4\pi^2} \int_{\Omega} \sum_{n \in \mathbb{Z}^2} S_{\nu}(\omega - 2n\rho) d\omega. \quad (6)$$

Since we are sampling at the Nyquist rate we do not observe any signal distortion in this case.

### 3.2. Mobile sampling with ideal LPF

If the mobile sensors use the ideal sinc filter as the LPF prior to sampling, the effective two-dimensional sampling kernel is given by  $h_s(x, y) = \frac{\rho}{\pi} \text{sinc}\left(\frac{\rho x}{\pi}\right) \delta(y)$  which is equivalently given in the Fourier domain by,

$$H_s(\omega) = \begin{cases} 1 & \text{for } 0 \leq |\omega_x| \leq \rho \\ 0 & \text{else.} \end{cases} \quad (7)$$

We note that the filter  $H_s$  is frequency limited in the x-direction. Further, since the spacing between the trajectories is equal to the Nyquist interval  $\Delta_y = \frac{\pi}{\rho}$  it follows that as long as the sampling interval along the trajectories satisfies  $\Delta_x < \frac{\pi}{\rho}$ , we have the following expression for the noise variance  $\sigma_{m1}^2$ :

$$\sigma_{m1}^2 = \frac{1}{4\pi^2} \int_{\Omega} \sum_{n \in \mathbb{Z}} S_{\nu}(\omega - (0, 2n\rho)^T) d\omega. \quad (8)$$

Comparing the expressions (6) and (8) we see that in the case of mobile sampling, only spectral shifts at lattice points along the x-axis contribute to the noise variance whereas in the case of static sampling spectral shifts from all points in the two-dimensional lattice contribute to the noise signal spectrum. The exact value of the reduction in noise variance obtained with mobile sampling can be computed if the true noise spectrum  $S_{\nu}(\cdot)$  is known.

### 3.3. Mobile sampling with box filter

In the case of mobile sampling with the box filter, we expect some distortion in the reconstruction because the filter response is not flat in the pass-band. The effective two-dimensional sampling kernel in this case is  $h_s(x, y) = \text{box}_{\Delta_b}(x) \delta(y)$  where

$$\text{box}_{\Delta_b}(x) := \begin{cases} \kappa & |x| < \Delta_b \\ 0 & \text{else} \end{cases}$$

where  $2\Delta_b$  denotes the spatial width of the box-filter response and  $\kappa = (2\rho)^{\frac{1}{2}} \left[ \frac{\Delta_b^2}{\pi^2} \int_{-\rho}^{\rho} \text{sinc}^2\left(\frac{\Delta_b \omega}{\pi}\right) d\omega \right]^{-\frac{1}{2}}$ . The sampling kernel is equivalently given in the Fourier domain by

$$H_s(\omega) = \frac{\kappa \Delta_b}{\pi} \text{sinc}\left(\frac{\Delta_b \omega_x}{\pi}\right). \quad (9)$$

The choice of  $\kappa$  ensures that  $\int_{\Omega} H_s(\omega)^2 d\omega = 4\rho^2$  which is consistent with the responses in (5) and (7).

Since the box filter is a non-ideal LPF, we expect some distortion in the reconstructed field. As before, let us assume that  $\Delta_x < \frac{\pi}{\rho}$  and that  $\Delta_y = \frac{\pi}{\rho}$ . Let  $F$  denote the Fourier transform of the bandlimited field being sampled and  $\hat{F}$  denote the Fourier transform of the reconstruction obtained by using an ideal reconstruction filter of the form (3). We have

$$\hat{F}(\omega) = \frac{\kappa \Delta_b}{\pi} F(\omega) \text{sinc}\left(\frac{\Delta_b \omega_x}{\pi}\right), \quad \omega \in \Omega. \quad (10)$$

Clearly, we see that the reconstructed field is a distorted version of the original field even in the absence of noise. The amount of distortion introduced for a given  $F$  can be computed using relation (10). We can also quantify the variance  $\sigma_{m2}^2$  of the noise in the reconstruction using relations (9) and (4):

$$\sigma_{m2}^2 = \frac{\kappa^2 \Delta_b^2}{4\pi^4} \int_{\Omega} \sum_{n \in \mathbb{Z}^2} S_{\nu}(\omega - \left(\frac{2n_x \pi}{\Delta_x}, 2n_y \rho\right)^T) \text{sinc}^2\left(\frac{\Delta_b}{\pi}(\omega_x - \frac{2\pi n_x}{\Delta_x})\right) d\omega.$$

Since it is inexpensive to increase the sampling rate used by each moving sensor, we can let  $\Delta_x \rightarrow 0$ , whence we obtain,

$$\sigma_{m2}^2 = \frac{\kappa^2 \Delta_b^2}{4\pi^4} \int_{\Omega} \sum_{n \in \mathbb{Z}} S_{\nu}(\omega - (0, 2n\rho)^T) \text{sinc}^2\left(\frac{\Delta_b \omega_x}{\pi}\right) d\omega. \quad (11)$$

If we now also allow  $\Delta_b \rightarrow 0$ , it is easy to see that  $\frac{\kappa \Delta_b}{\pi} \rightarrow 1$ . Hence the reconstruction in (10) becomes accurate and the expression in (11) reduces to that in (8). This means that we have  $\lim_{\Delta_b \rightarrow 0} \hat{F}(\omega) = F(\omega)$  for  $\omega \in \Omega$ , and  $\lim_{\Delta_b \rightarrow 0} \lim_{\Delta_x \rightarrow 0} \sigma_{m2}^2 = \sigma_{m1}^2$ . This means that if the sensors oversample at high rates along their path and use a rectangular LPF with a short impulse response, we can recreate the performance with an ideal LPF and Nyquist sampling.

We note that if the noise spectral density were white (i.e.  $S_{\nu}(\omega) = 1$  for all  $\omega \in \mathbb{R}^2$ ), then the expressions for the variance in (6), (8) and (11) tend to infinity since unfiltered white noise samples have infinite variance. However, in practice environmental noise is never completely white. We have the following result.

**Proposition 3.1.** *Suppose the noise spectral density  $S_{\nu}(\cdot)$  takes a value of unity on the set  $[-v\rho, v\rho] \times [-v\rho, v\rho]$  and 0 elsewhere for some  $\rho > 0$ . If  $v$  is an odd number then the variances in (6) and (8) reduce to*

$$\sigma_{stat}^2 = \frac{\rho^2 v^2}{\pi^2}, \quad \text{and} \quad \sigma_{m1}^2 = \frac{\rho^2 v}{\pi^2}.$$

Thus if the noise spectrum is flat with a bandwidth along each dimension equal to  $v$  times the field bandwidth, then we obtain a reduction in noise variance by a factor of  $v$  when we employ mobile sampling in place of static sampling.

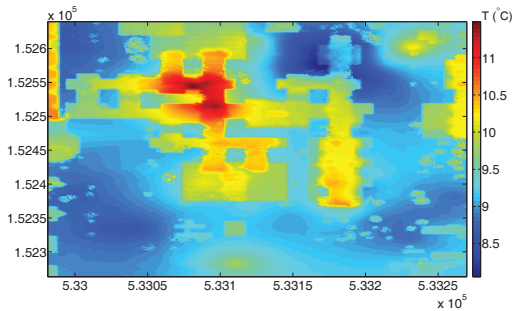


**Fig. 2.** Spatial temperature field on EPFL campus.

**Table 1.** Reconstruction errors with various schemes.

Data type	Static sensing	Mobile sensing	Mobile sensing with oversampling
Temperature	0.53%	0.45%	0.42% (no filter)
Simulated (SNR 20 dB)	9.9%	1.5%	1.5% (with filter)

#### 4. SIMULATIONS: MERITS OF MOBILE SENSING

We calculated the reconstruction accuracies that can be obtained using static and mobile sampling schemes for measuring the temperature field on the EPFL campus (Figure 2) obtained from [3]. For static sensing, we considered sensors on a rectangular grid as in Section 2.2. For mobile sensing we assumed that the sensors move parallel to the  $x$ -axis and apply an anti-aliasing filter prior to sampling. They take samples at the same points on the rectangular grid as in the static case. The percentage  $L^2$ -error in the reconstructed fields obtained via sinc-interpolation are shown in Table 1. The third column represents the performance obtained with mobile sensing assuming that the sensors measure the field at all points on their paths without any filtering. As the values in the table indicate, mobile sampling outperforms static sampling, and oversampling along the trajectories improves the performance further. The filtering operation in the mobile sampling scheme reduces the amount of aliasing in the samples leading to a reduction in the reconstruction error. We note that the temperature field is not truly bandlimited and hence the performance gains are more modest than what could be expected if the field were truly bandlimited.

In the second row of Table 1 we consider the same scheme for sampling and reconstructing a simulated bandlimited field in noise with spectra as in Proposition 3.1, with the ratio of the sides  $\nu = 40$ . For such a field we see from the values shown in Table 1 that the reduction in the average reconstruction error obtained with mobile sensing is more significant. We also see that the ratio of the errors under the static and mobile reconstruction schemes is approximately  $\nu^{\frac{1}{2}}$  as expected by the result of Proposition 3.1. In this example we allow filtering in the oversampling scheme since the field of interest is band-

limited. We see that in this case there is no improvement in the reconstruction accuracy with oversampling. This is because there is no advantage in increasing the sampling rate beyond the Nyquist rate.

#### 5. CONCLUSION AND FUTURE WORK

We have analyzed the advantages of mobile sensing over static sensing. Our results clearly demonstrate and quantify the SNR improvement while using time domain anti-aliasing filtering together with mobile sensing. In practice, it is possible that the physical process of moving the sensor through the field may affect the characteristics of the field or introduce noise and irregularities in the sensing process. In future work, these effects must also be taken into account to completely characterize the advantages of mobile sensing over static sensing in practice. Further investigation is required to study mobile sampling schemes for time-varying fields and non-bandlimited fields.

#### 6. REFERENCES

- [1] D. P. Petersen and D. Middleton, "Sampling and Reconstruction of Wave-Number-Limited Functions in N-Dimensional Euclidean Spaces," *Inform. Contr.*, vol. 5, pp. 279–323, 1962.
- [2] B. Rafaely, B. Weiss, and E. Bachmat, "Spatial aliasing in spherical microphone arrays," *IEEE Trans. Signal Process.*, vol. 55, no. 3, pp. 1003–1010, March 2007.
- [3] D. Nadeau, W. Brutsaert, M. Parlange, E. Bou-Zeid, G. Barrenetxea, O. Couach, M.-O. Boldi, J. Selker, and M. Vetterli, "Estimation of urban sensible heat flux using a dense wireless network of observations," *Environmental Fluid Mechanics*, vol. 9, pp. 635–653, 2009.
- [4] T. Ajdler, L. Sbaiz, and M. Vetterli, "Dynamic measurement of room impulse responses using a moving microphone," *J. Acoust. Soc. Am.*, vol. 122, no. 3, pp. 1636–1645, 2007.
- [5] A. Cigada, M. Lurati, F. Ripamonti, and M. Vanali, "Moving microphone arrays to reduce spatial aliasing in the beamforming technique: theoretical background and numerical investigation," *J. Acoust. Soc. Am.*, vol. 124, no. 6, pp. 3648–3658, 2008.
- [6] M.A. Richards, *Fundamentals of Radar Signal Processing*, McGraw-Hill, New York, 2005.
- [7] A. Singh, R. Nowak, and P. Ramanathan, "Active learning for adaptive mobile sensing networks," in *Proceedings of Information Processing in Sensor Networks (IPSN), 2006*, 2006.
- [8] S. Srinivasan and K. Ramamritham, "Contour estimation using collaborating mobile sensors," in *Proceedings of the 2006 workshop on dependability issues in wireless ad hoc networks and sensor networks*, New York, NY, USA, 2006, DIWANS '06, pp. 73–82, ACM.
- [9] J. Unnikrishnan and M. Vetterli, "Sampling High-Dimensional Bandlimited Fields on Low-Dimensional Manifolds," submitted to *IEEE Trans. Inf. Theory*, Nov. 2011.